Prediction of delamination crack growth in Carbon/Fiber Epoxy composite laminates using non-local interface damage model

Hassan ijaz[1,a], Muhammad Asad[1], Laurent Gornet[2], Syed Yasir Alam[2]
[1] School of Engineering, University of Management and Technology, Lahore, Pakistan
[2]GeM-UMR-CNRS 6183, Ecole Centrale de Nantes – 1 Rue de la Noë, BP 92101, 44321 Nantes Cedex 3, France
[a]Corresponding Author: hassan605@yahoo.com

***Abstract*—**The use of composite laminates is increasing in these days due to desired directional properties and low densities in comparison of metals. Delamination is a major source of failure in composite laminates where a crack like entity can initiate and propagate between different layers of composite laminates under given loading conditions. Damage mechanics based theories are employed to simulate the delamination phenomena between composite laminates. These damage models are inherently local and can cause the concentration of stresses around the crack tip. In the present study integral type non-local damage formulation is proposed to avoid the localization problem associated to damage formulation. A comprehensive study is carried out for the selection of different non-local variables. Finite Element simulations based on proposed non-local damage models and classical local damage model are performed and results are compared with available experimental data for UD IMS/924 Carbon/fiber epoxy composite laminate.

Keywords: Non-local Modeling/Delamination/Laminate/Damage Mechanics/Finite Element Analysis

1 Introduction

Composite laminates are used as a major load bearing structural parts in different industries like avionic and automobile. The driving force behind the increasing use of composite materials is high strength to weight ratio and directional properties. The composite laminates consist of different layers of fibers/fabric stacked together and cured with thermosetting resin [1]. Due to their inherent laminate nature, any two adjacent layers of composite laminates can separate due presence of delamination crack and may fail under given loading conditions [2-3].

In order to simulate the delamination crack growth in composite laminates, interface modeling techniques are developed using damage and fracture mechanics failure theories under static and fatigue loadings [4-7]. A lot of work has been carried out at the meso-scale (layers and interfaces) to understand the delamination failure process. Meso-scale, which lies between micro and macro scale consists of two basic constituents, layers and interfaces. The interlaminar interface, which is a mechanical surface, connects two adjacent layers and depends on the relative orientation of their fibres [8-9].

Localization is a common phenomenon associated to already available classic damage models [10-11]. Localization can cause the concentration of simulated results to certain regions rather a realistic and uniform distribution. One way to avoid localization is to introduce rate dependant damage modeling [12]. In recent times much attention is made to integral type non-local damage modeling in order to reduce the localization effects. This type of modeling is effectively discussed and employed to study the delamination crack growth in composite laminates [13-14].

In the present study a classical damage model proposed by Allix et al. is further modified to as no-local damage model [8]. In integral type non-local damage modeling, one variable is chosen for averaging of the results using Gaussian distribution function. For interlaminar interface damage modeling, three different types of variables like interfacial displacement "U", damage variable "d" and damage energy release rate "Y_d" are available for non-local damage formulation [14]. Finite element simulations on delamination crack growth with different types of non-local variables are performed and compared with each other and with classical local damage model in the present study. All the mathematical details regarding formulation of non-local modeling is comprehensively discussed and presented in this study.

This paper is organized as follows: Classical local damage model is presented in section 2. Proposed non-local interface damage modeling is detailed in section 3. Section 4 covers the finite element simulations of mode I delamination crack growth based on classical local and proposed non-local damage models for Carbon/fiber epoxy composite laminate. Finally, some concluding remarks are given in section 5.

2 Local Damage Evolution Law

.The interface is a two-dimensional surface entity that ensures the transfer of stress and displacement between two adjacent plies [4] [8]. This model coupled with the damage mechanics theory can take into account the phenomena of delamination that may occur during mechanical loading of structural parts. The relative displacement of one layer to other layer can be written as [8]:

$$U = U^{+} - U^{-} = U_1 N_1 + U_2 N_2 + U_3 N_3 \qquad (1)$$

Here, U^+ and U^- are displacement vectors on the top and bottom surfaces. Let the bisectors of the fiber direction be N_1 and N_2. The direction N_3 is normal to the interface, Figure 1.

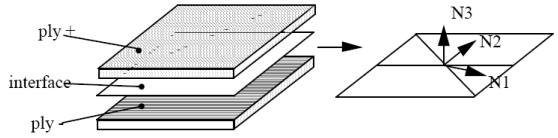

Fig. 1. Orthotropic directions of interface

The deterioration of the interface is taken into account by three internal damage variables d_1, d_2 and d_3. Here d_3 is associated with the opening mode (or mode I) and d_1, d_2 are associated with two shearing modes (mode II and mode III) of the interface.

The relationship between stress and displacement in orthotropic plane of axis can be expressed as:

$$\begin{pmatrix}\sigma_{13}\\ \sigma_{23}\\ \sigma_{33}\end{pmatrix}=\begin{pmatrix}k_1^0(1-d_1) & 0 & 0\\ 0 & k_2^0(1-d_2) & 0\\ 0 & 0 & k_3^0(1-d_3)\end{pmatrix}\begin{pmatrix}U_1\\ U_2\\ U_3\end{pmatrix} \quad (2)$$

Where k_1^0, k_2^0 and k_3^0 are interface rigidities associated to damage variables in orthogonal directions. Three different damage variables can be distinguished according to three modes of failure. The thermodynamic forces combined with the variables of damage and associated to the three modes of delamination are [8]:

$$\begin{cases} Y_{d_3}=\dfrac{1}{2}\dfrac{\langle\sigma_{33}\rangle_+^2}{k_3^0(1-d_3)^2} \quad Y_{d_1}=\dfrac{1}{2}\dfrac{{\sigma_{13}}^2}{k_1^0(1-d_1)^2} \\ Y_{d_2}=\dfrac{1}{2}\dfrac{{\sigma_{32}}^2}{k_2^0(1-d_2)^2} \end{cases} \quad (3)$$

Where, $\langle X\rangle_+$ represents the positive part of X. The energy dissipated in this model can be written as:

$$\Phi=Y_{d_1}\dot{d}_1+Y_{d_2}\dot{d}_2+Y_{d_3}\dot{d}_3 \qquad (\Phi\geq 0) \quad (4)$$

Three different damage variables corresponding to three modes of failure are strongly coupled and are governed by equivalent single energy release rate function as follows [15]:

$$\underline{Y}(t)=Max|_{\tau\leq t}\left(\left(\left(Y_{d_3}\right)^\alpha+\left(\gamma_1 Y_{d_1}\right)^\alpha+\left(\gamma_2 Y_{d_2}\right)^\alpha\right)^{1/\alpha}\right) \quad (5)$$

Where, γ_1 and γ_2 are coupling parameters and α is a material parameter which governs the damage evolution in mixed mode. The local damage evolution law is then defined by the choice of a material function as follows [15]:

$$\begin{aligned} &\textit{if} \quad \left[(d_3<1)\ \textit{and}\ (\underline{Y}<Y_R)\right]\\ &\textit{then}\\ &\qquad d_1=d_2=d_3=\omega(\underline{Y})\\ &\textit{else}\\ &\qquad d_1=d_2=d_3=1 \end{aligned} \quad (6)$$

The damage function is selected of the form [8] [15]:

$$\omega(\underline{Y})=\left[\frac{n}{n+1}\frac{\langle\underline{Y}-Y_O\rangle_+}{Y_C-Y_O}\right]^n \quad (7)$$

Where

Where, Y_O is threshold damage energy, Y_C is critical damage energy, n is Characteristic function of material (higher values of n corresponds to brittle interface) and Y_R is energy corresponding to rupture and can be expressed as: $Y_R=Y_O+\dfrac{n+1}{n}d^{1/n}\left(Y_C-Y_O\right)$.

A simple way to identify the propagation parameters (Y_C,γ_1,γ_2) is to compare the mechanical dissipation yielded by two approaches of Damage Mechanics and Linear Elastic Fracture Mechanics (LEFM). In the case of pure mode situations, when the critical energy release rate reaches its stabilized value at the propagation denoted by G_C, comparison of dissipations between Fracture Mechanics and Damage Mechanics approaches lead to [15]:

$$G_{IC}=Y_C;\ G_{IIC}=\frac{Y_C}{\gamma_1};\ G_{IIIC}=\frac{Y_C}{\gamma_2} \quad (8)$$

In order to satisfy the energy balance principle of LEFM, the area under the curve of stress-displacement curve for the whole debonding process (DP) obtained through Damage Mechanics formulation is set equal to critical energy release rate G_{iC}, and the following relations for the mode I, mode II and mode III critical energy release rates can be written:

$$G_{IC}=\int_{DP}\sigma_{33}\,dU_3,\quad G_{IIC}=\int_{DP}\sigma_{13}\,dU_1,\quad G_{IIIC}=\int_{DP}\sigma_{23}\,dU_2 \quad (9)$$

The area under the curve will always equal to critical energy G_C for any mode of delamination, see Figure 2. For mixed-mode loading situation, a standard LEFM model is recovered as [15]:

$$\left(\frac{G_I}{G_{IC}}\right)^\alpha+\left(\frac{G_{II}}{G_{IIC}}\right)^\alpha+\left(\frac{G_{III}}{G_{IIIC}}\right)^\alpha=1 \quad (10)$$

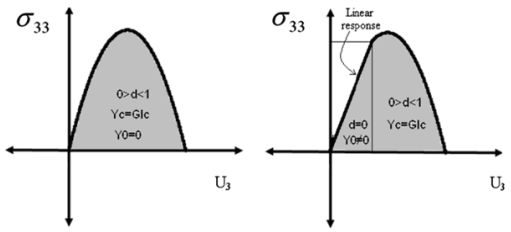

Fig. 2. Interfacial Stress vs Disp curve for mode I

3 Non-Local Interface Damage Model

Damage models need to describe strain-softening behavior in order to characterize microscopic degradation processes. A phenomenon called "localization" occurs in structural analyses with strain-softening models. Regularization techniques are therefore essential in

Damage Mechanics. The goal of using these techniques is to control the localization. In order to control the localization problem some authors proposed rate-dependent [12] and gradient enhanced [11] damage models. However, in this paper an integral type non-local damage model is proposed. Basically, three different types of non-local models are proposed in this section and their details are given below.

Averaging The Damage Variable "d"

In this type of non-local damage model, the damage variable d is made non-local by means of a spatial averaging over the surrounding domain V with respect to weight function α_0 [16]:

$$\bar{d}(x) = \frac{1}{V_r(x)} \int_V \alpha_0 \left(\|x - \zeta\| \right) d(\zeta) d\zeta \tag{11}$$

Where

$$V_r(x) = \int_V \alpha_0 \left(\|x - \zeta\| \right) d\zeta \tag{12}$$

Here the damage variable d which is made non-local through above equations is calculated initially from Eq. (6). An isotropic function such as Gaussian distribution function is chosen as weight function over the domain V [13].

$$\alpha_0(r) = \exp\left(-\frac{r^2}{2l^2} \right) \tag{13}$$

This weight function depends on the distance $r = \|x - \zeta\|$ between points x and ζ and on a parameter l called the internal length scale. This quantity represents a measure of the non-local averaging. The distribution of α_0 with respect to distance r, where $r = \|x - \zeta\|$, is shown in Figure 3.

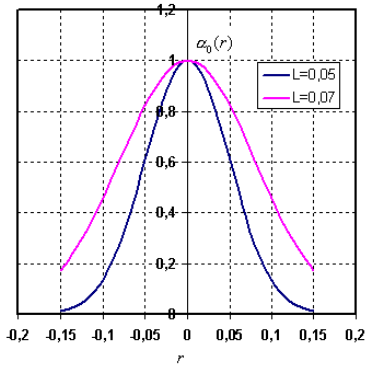

Fig. 3. Distribution of weight function

Averaging The Variable Y_{di} $(i = 1,2,3)$

Now take the damage energy release rates Y_{di} $(i = 1,2,3)$ correspond to three failure modes, see Eq. (3). Now one can write

$$\overline{Y_{di}}(x) = \frac{1}{V_r(x)} \int_V \alpha_0 \left(\|x - \zeta\| \right) Y_{di}(\zeta) d\zeta \tag{14}$$

Now $V_r(x)$ can be calculated using Eq. (12). Once the value of $\overline{Y_{di}}(x)$ is known for three failure modes then non-local damage variable d can be calculated as a function of $\overline{Y_{di}}(x)$ i.e. $d = d(\underline{Y}(\overline{Y_{di}}(x)))$. Here $\underline{Y}$ is the equivalent damage energy release rate. Once the value of equivalent $\underline{Y}$ is known using non-local $\overline{Y_{di}}(x)$ variables, one can calculate damage variable d using Eq. (6).

Averaging The Relative Displacement U_i $(i = 1,2,3)$

Another approach can be used by averaging the relative interface displacement expressed through Eq. (1):

$$\overline{U_i}(x) = \frac{1}{V_r(x)} \int_V \alpha_0 \left(\|x - \zeta\| \right) U(\zeta) d\zeta \tag{15}$$

Now again $V_r(x)$ can be calculated using equation (12). Once the value of $\overline{U_i}(x)$ is known then non-local damage variable d can be calculated as a function of $\overline{U_i}(x)$ i.e. $d = d(Y(\overline{U}_i(x)))$.

1 Compute $Y_{d_i\,n+1}$

$$Y_{d_3 n+1}(\zeta) = \frac{1}{2} k_3^0 < U_3(\zeta) >_{+\,n+1}^2$$

$$Y_{d_2 n+1}(\zeta) = \frac{1}{2} k_2^0 (U_2(\zeta))_{n+1}^2 \qquad Y_{d_1 n+1}(\zeta) = \frac{1}{2} k_1^0 (U_1(\zeta))_{n+1}^2$$

2 Compute $\underline{Y}_{n+1}$

$$\underline{Y}_{n+1} = Sup|_{\tau \le t} \left[\left(\left(Y_{d_3 n+1} \right)^\alpha + \left(\gamma_1 Y_{d_1 n+1} \right)^\alpha + \left(\gamma_2 Y_{d_2 n+1} \right)^\alpha \right)^{1/\alpha} \right]$$

3 Compute $\omega(\underline{Y}_{n+1})$

4 Compute damage variables $\bar{d}_1, \bar{d}_2, \bar{d}_3$

$$d_{1n+1}(\zeta) = \omega(\underline{Y}_{n+1}) \qquad d_{2n+1}(\zeta) = \omega(\underline{Y}_{n+1})$$

$$d_{3n+1}(\zeta) = \omega(\underline{Y}_{n+1})$$

$$\bar{d}_{3n+1}(x) = \frac{\sum \alpha_0 \left(\|x - \zeta\| \right) d_{3n+1}(\zeta)}{\sum \alpha_0 \left(\|x - \zeta\| \right)} \qquad \bar{d}_{2n+1}(x) = \frac{\sum \alpha_0 \left(\|x - \zeta\| \right) d_{2n+1}(\zeta)}{\sum \alpha_0 \left(\|x - \zeta\| \right)}$$

$$\bar{d}_{1n+1}(x) = \frac{\sum \alpha_0 \left(\|x - \zeta\| \right) d_{1n+1}(\zeta)}{\sum \alpha_0 \left(\|x - \zeta\| \right)} \quad \text{with} \quad \alpha_0(r) = \exp\left(-\frac{r^2}{2l^2} \right)$$

5 Compute stresses

$$\sigma_{33n+1} = k_3^0 (1 - \bar{d}_{3n+1})(U_3)_{n+1} \qquad \sigma_{23n+1} = k_2^0 (1 - \bar{d}_{2n+1})(U_2)_{n+1}$$

$$\sigma_{13n+1} = k_1^0 (1 - \bar{d}_{1n+1})(U_1)_{n+1}$$

6 Update and exit

Table 1. d based Non-Local damage model implementation

4. Finite Element Simulations

The proposed non-local damage models presented here are implemented in Cast3M (CEA) finite element code. For the study of delamination, a special interface element of zero thickness has been used [17], which is already implemented in finite element software CAST3M [18]. A four node zero thickness interface element "JOI2" available in CAST3M library [18] is used in the finite element analysis. The "JOI2" element has 2dof/node and

two Gauss points of integration per element. Implementation of three different non-local damage evolution laws are made in CAST3M via procedure PERSO1 and using subroutine UMAT [18]. The finite element implementations of all non-local damage models are given in Tables 1 to 3.

1 Compute $\underline{Y}_{n+1}$

with

$$Y_{d_3\,n+1}(\zeta)=\frac{1}{2}k_3^0<U_3(\zeta)>_{+\,n+1}^2$$

$$Y_{d_2\,n+1}(\zeta)=\frac{1}{2}k_2^0(U_2(\zeta))_{n+1}^2 \qquad Y_{d_1\,n+1}(\zeta)=\frac{1}{2}k_1^0(U_1(\zeta))_{n+1}^2$$

$$\overline{Y}_{d_3\,n+1}(x)=\frac{\sum\alpha_0\left(\|x-\zeta\|\right)Y_{d3n+1}(\zeta)}{\sum\alpha_0\left(\|x-\zeta\|\right)} \qquad \overline{Y}_{d_2\,n+1}(x)=\frac{\sum\alpha_0\left(\|x-\zeta\|\right)Y_{d2n+1}(\zeta)}{\sum\alpha_0\left(\|x-\zeta\|\right)}$$

$$\overline{Y}_{d_1\,n+1}(x)=\frac{\sum\alpha_0\left(\|x-\zeta\|\right)Y_{d1n+1}(\zeta)}{\sum\alpha_0\left(\|x-\zeta\|\right)} \quad with \quad \alpha_0(r)=\exp\left(-\frac{r^2}{2l^2}\right)$$

2 Compute $\underline{Y}_{n+1}$

$$\underline{Y}_{n+1}=Sup|_{\tau\le t}\left[\left(\left(\overline{Y}_{d_3\,n+1}\right)^{\alpha}+\left(\gamma_1\overline{Y}_{d_1\,n+1}\right)^{\alpha}+\left(\gamma_2\overline{Y}_{d_2\,n+1}\right)^{\alpha}\right)^{1/\alpha}\right]$$

3 Compute $\omega(\underline{Y}_{n+1})$

4 Compute damage variables d_1, d_2, d_3

$$d_{1n+1}=\omega(\underline{Y}_{n+1}) \qquad d_{2n+1}=\omega(\underline{Y}_{n+1})$$

$$d_{3n+1}=\omega(\underline{Y}_{n+1})$$

5 Compute stresses

$$\sigma_{33n+1}=k_3^0(1-d_{3n+1})(U_3)_{n+1} \qquad \sigma_{23n+1}=k_2^0(1-d_{2n+1})(U_2)_{n+1}$$

$$\sigma_{13n+1}=k_1^0(1-d_{1n+1})(U_1)_{n+1}$$

6 Update and exit

Table 2. Y_d based Non-Local damage model implementation

1 Compute $Y_{d_1\,n+1}$

with

$$(\overline{U_3}(x))_{n+1}=\frac{\sum\alpha_0\left(\|x-\zeta\|\right)(U_3(\zeta))_{n+1}}{\sum\alpha_0\left(\|x-\zeta\|\right)} \qquad (\overline{U_2}(x))_{n+1}=\frac{\sum\alpha_0\left(\|x-\zeta\|\right)(U_2(\zeta))_{n+1}}{\sum\alpha_0\left(\|x-\zeta\|\right)}$$

$$(\overline{U_1}(x))_{n+1}=\frac{\sum\alpha_0\left(\|x-\zeta\|\right)(U_1(\zeta))_{n+1}}{\sum\alpha_0\left(\|x-\zeta\|\right)} \quad \text{with} \quad \alpha_0(r)=\exp\left(-\frac{r^2}{2l^2}\right)$$

$$Y_{d_3\,n+1}=\frac{1}{2}k_3^0<\overline{U_3}(x)>_{+\,n+1}^2$$

$$Y_{d_2\,n+1}=\frac{1}{2}k_2^0(\overline{U_2}(x))_{n+1}^2 \qquad Y_{d_1\,n+1}=\frac{1}{2}k_1^0(\overline{U_1}(x))_{n+1}^2$$

2 Compute $\underline{Y}_{n+1}$

$$\underline{Y}_{n+1}=Sup|_{\tau\le t}\left[\left(\left(Y_{d_3\,n+1}\right)^{\alpha}+\left(\gamma_1 Y_{d_1\,n+1}\right)^{\alpha}+\left(\gamma_2 Y_{d_2\,n+1}\right)^{\alpha}\right)^{1/\alpha}\right]$$

3 Compute $\omega(\underline{Y}_{n+1})$

4 Compute damage variables d_1, d_2, d_3

$$d_{1n+1}=\omega(\underline{Y}_{n+1}) \qquad d_{2n+1}=\omega(\underline{Y}_{n+1})$$

$$d_{3n+1}=\omega(\underline{Y}_{n+1})$$

5 Compute stresses

$$\sigma_{33n+1}=k_3^0(1-d_{3n+1})(U_3)_{n+1} \qquad \sigma_{23n+1}=k_2^0(1-d_{2n+1})(U_2)_{n+1}$$

$$\sigma_{13n+1}=k_1^0(1-d_{1n+1})(U_1)_{n+1}$$

6 Update and exit

Table 3. U based Non-Local damage model implementation

E_{11} (MPa)	138000
E_{22} (MPa)	1100
E_{33} (MPa)	100
υ_{12}	0.3434
G_{12} (MPa)	4400

Table 4. Mechanical properties of IMS/924 [18]

Test Method	G_C (KJ/m^2)	Interface properties
Mode I (DCB)	0.26 ± 0.01	$n=0.2,\ Y_C=0.26\pm0.01$ KJ/m^2 $K_0^3=1000$ MPa/mm

Table 5. Identified interface properties of IMS/924

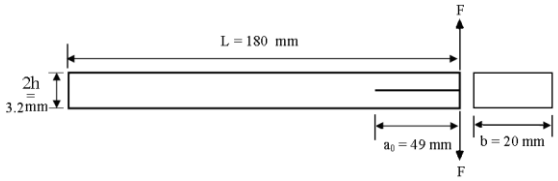

Fig. 4. Geometry of DCB specimen

Fig. 5. Mesh diagram of DCB specimen

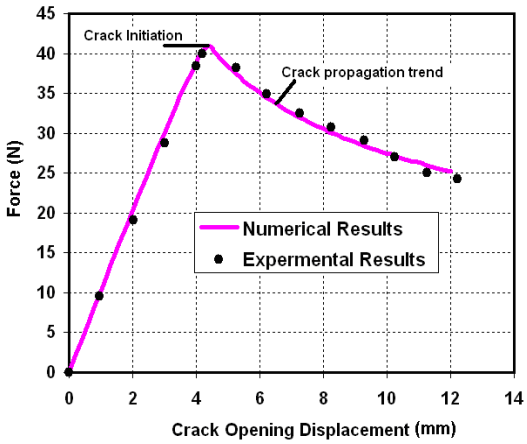

Fig. 6. Force vs Crack opening displacement curve for local damage model

Figure 7 shows the result of applied load versus delamination crack opening displacement for "d" based non-local formulations. The effect of internal length parameter l can be observed in the Figure 8. From figure it can be concluded that non-local damage evolution law behaves like local one for small values of l. This is because for small values of l there will be fewer elements available for making the average of damage variable d. The good value of l can be found from experiments by closely observing the delamination crack front because this material length l defines the size of interaction zone of damage localization [20-21]. As the value of l increases the crack initiation point moves farther away and then drops after the crack propagation has started but this crack propagation portion of the curve stabilizes a bit higher in comparison to smaller values of l, see Figure 7.

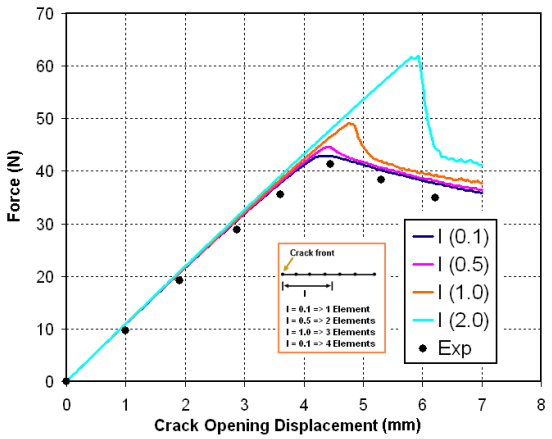

Fig. 7. Force vs Crack opening displacement curve for "d" based non-local model

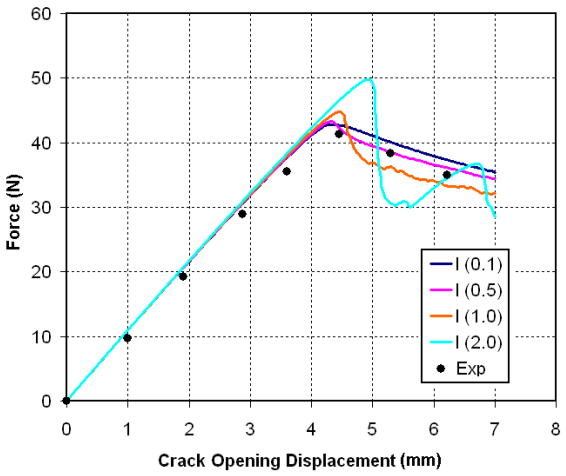

Fig. 8. Force vs Crack opening displacement curve for "Y_{di}" based non-local model

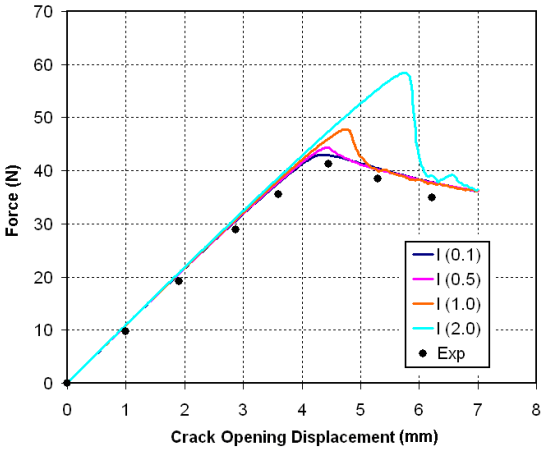

Fig. 9. Force vs Crack opening displacement curve for "U_i" based non-local model

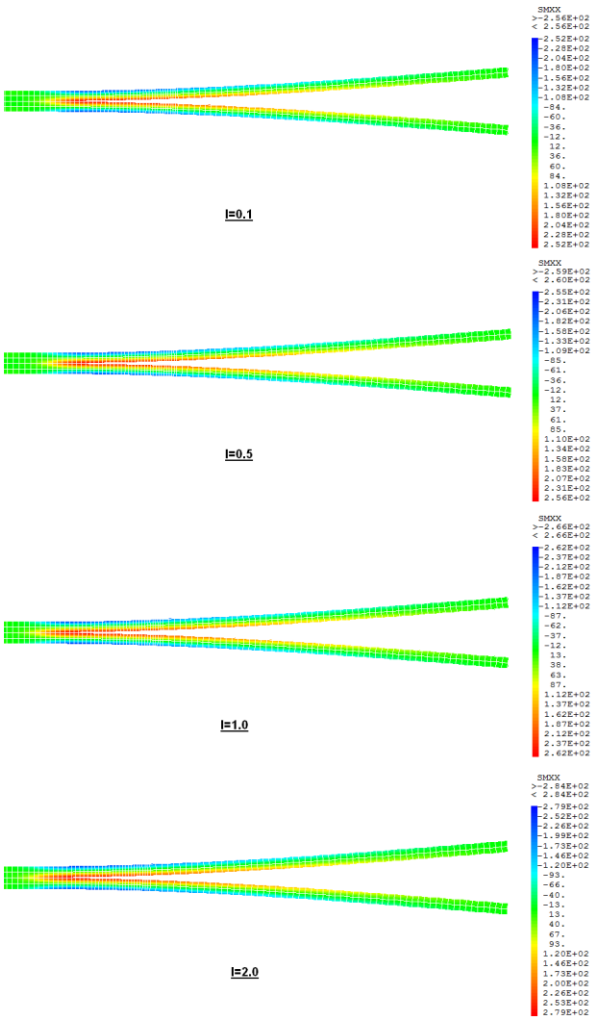

Fig. 10. In-plane stresses of DCB specimen for d based non-local damage model

Figure 8 shows the result of applied load versus delamination crack opening displacement for "Y_{di}" based non-local formulations. From Figure 8, it is clear that as the value of l increases, the crack initiation point also moves away but the crack propagation portion of the curve is not as stable as in previous case of "d" based non-local formulations. In fact, results can be considered quite erratic for "Y_{di}" based non-local formulations because of ups and downs of curves for different values of internal length parameter l.

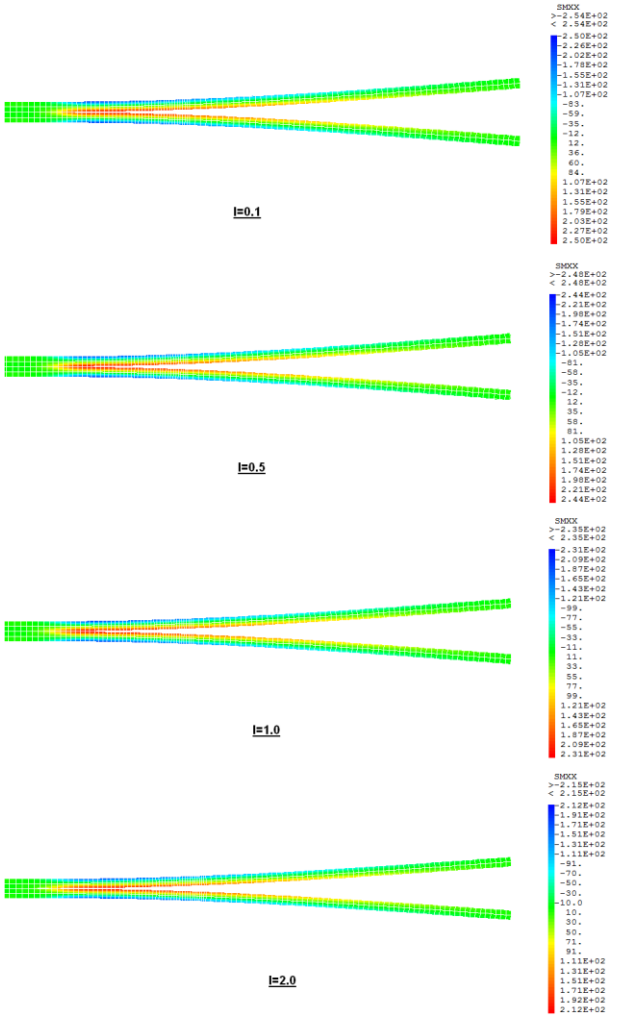

Fig. 11. In-plane stresses of DCB specimen for Y_d based non-local damage model

Similarly, Figure 9 shows the result of applied load versus delamination crack opening displacement for "U_i" based non-local formulations. The crack initiation phenomenon occurs in same way as for previous two cases i.e. shown increasing trend with the increase of internal length parameter l. But crack propagation portion of curve seems to be more stable than the previous two cases. In this case, crack propagation regions tend to conform each other for different values of length parameter l.

Figure 10 shows the in-plane stresses obtained from finite element analysis of DCB for "d" based non-local damage model for different values of internal length parameter l during crack propagation process. From Figure 10, one can observe the higher amount of stresses with increasing values of l that is also in accordance with results shown in figure 7.

Similarly Figure 11 presents the in-plane stresses during crack propagation of DCB specimen for "Y_d" based non-local damage model for different values of internal length parameter l. Contrary to "d" based finite element results, one can observe decreasing trend of stresses with increasing values of l. Figure 8 also shows similar trend for "Y_d" based non-local formulation, but Figure 8 also shows that reaction force varies erratically as value of l increases.

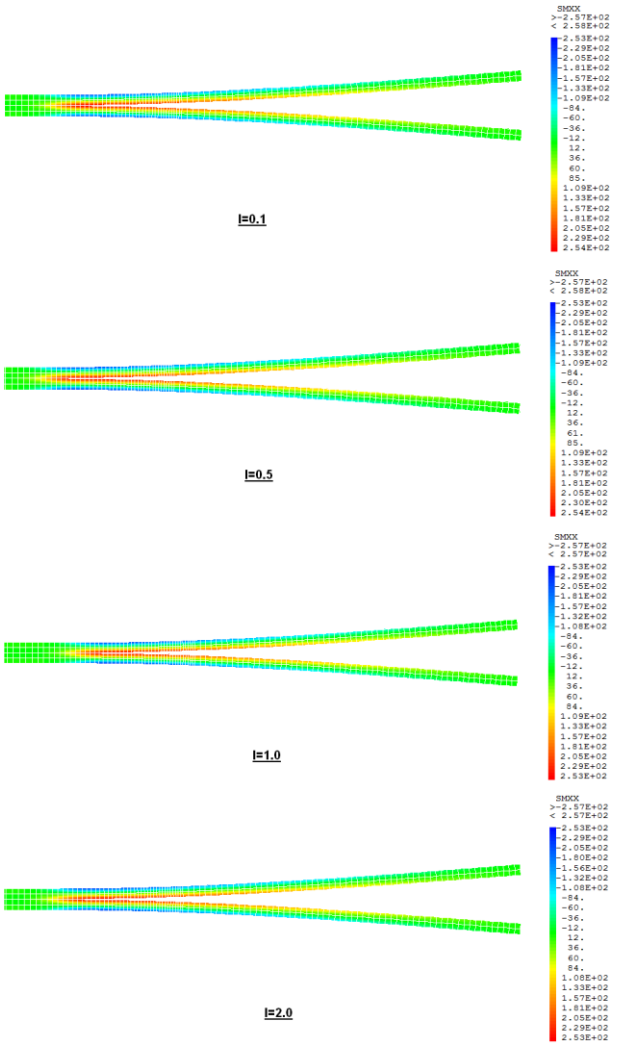

Fig. 12. In-plane stresses of DCB specimen for U based non-local damage model

5. Conclusion

In the present study, a classical local damage model presented by Allix et al. is further modified to incorporate the non-local effects. Three different non-local interface damage formulations based on averaging of variables d, Y_d and U are presented. Finite element simulations of IMS/924 composite laminate for mode I delamination crack growth are performed and results are compared with each other. From the finite element simulations it is clear that d and U based non-local damage models show much better results in comparison of Y_d based non-local formulation. For Y_d based non-local formulation, reaction force start varying erratically with increasing values of l. From finite element simulations, it is also clear that non-local modeling is strongly influenced by internal length parameter l. For smaller values of l, the results of local and non-local interface modeling are close to each other because few number of elements are available for averaging in non-local modeling with smaller value of l.

References

1. Herakovich CT. Mechanics of fibrous composites. 1st ed. New york: John Wiley & sons Inc, 1997.
2. Kenane M, Benzeggagh ML. Mixed-mode delamination fracture toughness of unidirectional glass/epoxy composites under fatigue loading. Composites Science and Technology, 57, 597-605, 1997.
3. Leif E Asp, Sjogren A, Greenhalgh ES. Delamination growth and thresholds in a carbon/epoxy composite under fatigue loading. Journal of Composite Technology and Research, 23(2), 55-68, 2001.
4. Allix O, Ladevèze P. Interlaminar interface modeling for the prediction of delamination. Composite Structures, 22, 235-242, 1992.
5. Chaboche JL, Girard R, Levasseur P. On the interface debonding models. International Journal of Damage Mechanics, 6, 220-257, 1997.
6. Davies P, Cantwell W, Moulin C, Kausch HH. A study of delamination resistance of IM6/PEEK composites. Composites Science and Technology, 36, 153-166, 1989.
7. Ijaz H, Gornet L, A high-cyclic elastic fatigue damage model for carbon fibre epoxy matrix laminates with different mode mixtures. Composites Part B: Engineering, 42, 1173- 1180, 2011.
8. Allix O, Ladevèze P, Gornet L, Léveque D, Perret L. A computational damage mechanics approach for laminates: identification and comparison with experimental results. Damage Mechanics in Engineering Materials, Studies in Applied Mechanics 46, G.Z. Voyiadjis, J.W. Ju & J.- L. Chaboche eds. Elsevier, 481-500, 1998.
9. Alfano G, Crisfield MA. Finite element interface models for the delamination analysis of laminated composites: mechanical and computational issues. International Journal for Numerical Methods in Engineering, 50, 1701-1736, 2001.
10. Bazant ZP, Pijaudier-Cabot G. Nonlocal continuum damage, localization instability and convergence. Journal of Applied Mechanics, 55, 287-293, 1988.
11. Peerlings RHJ, Geers MGD, De Borst R, Breckelmans WAM. A critical comparison of nonlocal and gradient enhanced softening continua. International Journal of Solids and Structures, 38, 7723-7746, 2001.
12. Marguet S, Rozycki P, Gornet L. A rate dependent constitutive model for carbon-fiber reinforced plastic woven fabric. Mechanics of Advanced Materials and Structures, 14, 619-631, 2007.
13. Borino G, Failla B, Parrinello F. Nonlocal elastic damage interface mechanical model. International Journal for Multiscale Computational Engineering, 5, 153-165, 2007.
14. Ijaz H, Gornet L, Khan MA, Saleem W, Nisar K, Chaudry SR. Prediction of delamination crack growth Carbon/fiber epoxy composite laminates using non-local cohesive zone modeling. Advanced Materials Research, 570, 25-36, 2012.
15. Ladevèze P, Corigliano A. Modeling and simulation of crack propagation in mixed-modes interlaminar fracture specimens. International Journal of Fracture, 77, 111-140, 1996.
16. Jirasek M. Nonlocal models for damage and fracture: comparison of approaches. International Journal of Solids and Structures, 35, 4133-4145, 1998.
17. Befr G. An isoparametric joint/interface element for finite element analysis. International Journal for Numerical Methods in Engineering, 21, 585-600, 1985.
18. Verpeaux P, Charras T, Millard A. Castem 2000 : Une approche moderne du calcul des structures, Calcul des Structures et Intelligence Artificielle (J.M. Fouet, P. Ladevèze, and R. Ohayon, eds.), 2, 227–261, 1988. http://wwwcast3m.cea.fr.
19. Cartié DDR. Effect of Z-fibres on the delamination behaviour of carbon fibre/ epoxy laminates. PhD thesis, Cranfield University UK, 2000.
20. Bazant ZP, Pijaudier-Cabot G. Measurement of characteristic length of nonlocal continuum. J Eng Mech, 115(4), 755-767, 1989.
21. Mohamad Hussein A, Shao JF. Modelling of elastoplastic behaviour with non-local damage in concrete under compression. Computers and Structures, 85, 1757-1768, 2007.